Eur Biophys J (2006) 35:663–674
DOI 10.1007/s00249-006-0075-5

ARTICLE

Unfolding time distribution of GFP by single molecule fluorescence spectroscopy

G. Chirico · F. Cannone · A. Diaspro

Received: 23 February 2006 / Revised: 5 May 2006 / Accepted: 18 May 2006 / Published online: 20 June 2006

Abstract We have studied the unfolding of single molecules of GFP-mut2 mutant trapped in wet silica gels in a wide range of GuHCl concentration. After the addition of denaturant, the number of fluorescent molecules decreases with unfolding rates (of the order of 0.01 min^{-1}) that are in very good agreement with bulk fluorescence and circular dichroism data. Unexpectedly, single molecule experiments show rare fluctuations in the number of fluorescent proteins at equilibrium. On the other hand, although a first approximate description of the number decays can be reasonably performed by single exponential functions, the distributions of the single molecule unfolding times show a maximum at times ≅ 50–100 min up to the denaturation midpoint concentration of [GuHCl] ≅ 2.5 M. A theoretical analysis of the distributions indicates that this feature is a fingerprint of the competition between unfolding and refolding processes when the protein is very far from the midpoint denaturant concentration.

Keywords GFP · Two photon microscopy · Single molecule · Protein unfolding

G. Chirico (✉) · F. Cannone
Department of Physics, University of Milano Bicocca, Piazza della scienza 3, Milano 20126, Italy
e-mail: chirico@mib.infn.it

A. Diaspro
LAMBS, MicroScoBiO Research Center and Department of Physics, University of Genoa, Via Dodecaneso 33, Genova 16146, Italy

G. Chirico · F. Cannone · A. Diaspro
INFM-CNR Istituto Nazionale per al Fisica della Materia and Centro Nazionale delle Ricerche, Genova, Italy

A. Diaspro
IFOM, The FIRC Institute for Molecular Oncology Foundation, Via Adamello 16, Milan 20139, Italy

Introduction

Complex dynamics is ubiquitous in biological systems, from single proteins (Baldini et al. 2005) to cells, where thermal fluctuations play an essential role. Protein folding is a complex process that encompasses several biological functions, from DNA–RNA driven transcription–translation events to protein synthesis and maturation. Investigations aimed at understanding the basic principles of protein folding and unfolding have appeared since early 1960's (Dill and Chan 1997; Onuchic et al. 1997) and have made use of theoretical (Lindorff-Larsen et al. 2005), experimental (Eaton et al. 2000; Myers and Oas 2002) and computational approaches (Kubelka et al. 2004).

The denaturation kinetics, which is modeled as a mono-molecular chemical reaction of the type $N \leftrightarrow U$, characterized by the unfolding, k_u, and the refolding, k_f, relaxation rates, is completely determined by the rate $\lambda = k_u + k_f$. This parameter is then evaluated from the relaxation rate of the (single exponential) decay of an optical signal, typically circular dichroism (CD) or fluorescence, versus time upon increasing or lowering of the denaturant concentration. The Chevron plot analysis proposed by Tanford is often adopted in unfolding and refolding studies of proteins (Tanford 1968). This approach is based on the assumption of a

linear relationship between the free energies of the different folding states and denaturant concentration (Tanford 1968). In some cases and even with small globular proteins, unfolding intermediates have been proposed and the protein unfolding kinetics has been the object of a detailed scrutiny (Went et al. 2004), aimed to reveal the occurrence of intermediates from the curvature of the Chevron plot (Matouschek et al. 1990). In general, for proteins that fold without populating an intermediate state, both arms of the chevron plot are linear (Jackson and Fersht 1991). However, the occurrence of folding intermediates might be visible also from a non-exponential trend of the optical signal decay, though this is hardly measurable in practice since it should be obtained from an accurate analysis of the first time derivative of the optical signal decay. A second practical concern must be raised when making use of Chevron plots in protein unfolding studies. Unfolding and refolding rates contribute equally to the total relaxation rate. However, it is difficult to determine simultaneously both k_f and k_u, from a denaturation or renaturation experiment only, due to the considerable unbalance between the unfolded and native populations that occurs as soon as the titration concentration falls far from the denaturation midpoint.

Single molecule techniques are good candidates to follow the complete folding/refolding pathways and to probe their variability (Baldini et al. 2005). Most of the studies presented in the literature were based on the observation of the molecules ''on-the-fly'', while diffusing in the excitation volume (Mayor et al. 2003; Lipman et al. 2003) or after immobilization within surface-tethered lipid (Rhoades et al. 2003) or in functionalized glasses (Chirico et al. 2002). In recent studies short peptides or small proteins labeled with two fluorescent probes were used to report internal movements via Förster resonance energy transfer (FRET) (Weiss 2000) and a considerable effort was also devoted to the analysis of potential artifacts (Mayor et al. 2003; Schuler et al. 2002; Talaga et al. 2000). Regarding unfolding studies, single molecule analysis would in principle offer the possibility to investigate the occurrence of intermediate states and to evaluate the effect of unfolding/refolding competition in the unfolding process by detecting the fluctuations in the number of folded and unfolded proteins.

The aim of this study is to explore the unfolding kinetics of single molecules of the GFP-mut2 mutant looking for possible non-exponential relaxations of the number of native proteins. GFP-mut2, a mutant of GFP containing a triple substitution, S65A, V68L, S72A (Cormack et al. 1996), was entrapped in wet nanoporous silica gels, an encapsulation procedure that perturb negligibly the protein overall rotational diffusion (Chirico et al. 2002) in its folded state. GfPmut2 has been chosen for the high fluorescence brightness and for the possibility to observe simultaneously the neutral and the anionic emission under two-photon excitation (Cannone et al. 2005b). Fluorescence signals, generated by the intrinsic GFP chromophore (Zimmer 2002), both on the neutral or the anionic state, were detected by two-photon microscopy (Cannone et al. 2005b) in order to follow GFPmut2 unfolding, In fact, the GFP chromophore remains intact in the denatured state, but fluorescence is lost upon disruption of the native topology (Talaga et al. 2000). We have previously shown, by comparison to bulk CD measurements in silica gels (Campanini et al. 2005), that the fluorescence bleaching of single GFP molecules (Cannone et al. 2005a) induced by the addition of GuHCl is correlated to the loss of the secondary structure.

The main result of the present manuscript, obtained through single molecule spectroscopy, is to show that rare fluctuations in the number of folded proteins can be detected in single molecule experiments, thereby preventing the possibility of a direct simultaneous measurement of k_f and k_u. This is a result that could not be obtained from bulk measurements. On the other hand, we show that the *single molecule* unfolding kinetics and the distribution of the single molecule unfolding times, has a non-exponential behavior at low denaturant concentrations in unfolding experiments. By developing a simple analysis of a two-state transition in non-equilibrium conditions we suggest that the observed non-exponential behavior can be taken as a fingerprint of the competition between refolding and unfolding kinetics in a situation of strong asymmetry between the unfolded and native protein population.

Experimental (materials and methods)

Chemicals and buffers

All chemicals were purchased from Sigma-Aldrich (St. Louis, MO, USA), except guanidinium hydrochloride (Fluka, Buchs, Swiss, p.n.50937), and were used without further purification. Experiments were carried out in 20 mM Tris–HCl, 600 mM NaCl, pH 6.6, at 37°C. Since silica gels bear a net negative charge at pH around neutrality (Shen and Kostic 1997), sodium chloride was added to the buffer to shield the gel matrix charges and avoid partitioning of the denaturant molecules between the pores of the gel and the surrounding medium (Badjic and Kostic 1999).

GFPmut2 expression and purification

GFPmut2 gene, cloned in a pKEN1 vector, was kindly provided by Dr. Brendan P. Cormack (Department of Microbiology and Immunology, Stanford University School of Medicine, Stanford, CA, USA) (Cormack et al. 1996). Protein expression and purification was carried out as previously described (Chirico et al. 2002). GFPmut2 stock solutions were dialyzed against 50 mM Tris buffer, pH 8.0, and kept at –80°C.

Protein encapsulation in silica gels

Encapsulation of GFPmut2 in silica gels was carried out according to Bettati and Mozzarelli (Bettati and Mozzarelli 1997). Two volumes of a solution containing GFPmut2 and 100 mM phosphate buffer, pH 7.5, were mixed with three volumes of a sol prepared by acid hydrolysis of tetramethyl orthosilicate (Ellerby 1992). The final GFPmut2 concentration was approximately 100 nM. About 2 μl of the mixture were deposited in a circular micro-chamber, ≅ 5 mm in diameter and ≅ 500 μm thick, built on a glass slide. Upon gelation, protein-doped silica gels were covered with 100 mM phosphate buffer, 1 mM DTT, 1 mM EDTA, pH 7 and stored at 4°C for at least 12 h before use.

Unfolding-refolding experiments

For denaturation experiments a stock solution containing 6 M guanidinum hydrochloride, 600 mM NaCl, 50 mM Tris, pH 6.6, was prepared. The stock solution was diluted with buffer to obtain the desired denaturant concentration. Unfolding and refolding experiments were carried out by rapidly rinsing silica gels doped with GFPmut2 with either a denaturant-containing or a denaturant-free solution. Axial and in-plane scanning ensured that the field under observation was unaltered during the long-lasting denaturation experiments. Solvent exchange was proved to occur in less than 2 s with gel thickness ≅ 400 μm as used here (Cannone et al. 2005a). This time delay cannot affect the time course of GFPmut2 unfolding that takes place in minutes or longer times (see below). All experiments were carried out at 37°C.

Optical setup

The two-photon excitation setup was based on a mode-locked Ti:sapphire lasers (Tsunami 3960, Spectra Physics, CA, USA) coupled with a Nikon (Japan) TE300 microscope. The laser provides ≅ 280 fs pulses on the sample plane (Cannone et al. 2003) at a repetition frequency of 80 MHz, in the range 720–950 nm. Optical collection is based on a scanning head PCM2000 (Nikon, Japan), adapted for two-photon excitation (Diaspro 2001). The radial and axial profiles are 240 ± 40 nm and 780 ± 50 nm, respectively. The excitation intensity on the sample is computed as the average power divided by the area of the point spread function in the focal plane.

Fluorescence imaging

The images (512 × 512 pixels) of encapsulated fluorescent protein molecules were acquired with a residence time of 3 μs per pixel, field of view ≅ 10 μm × 10 μm and excitation power on the sample of ≅ 1–15 MW/cm^2. With these parameters, one single molecule spot corresponds to approximately 11 × 11 pixels. The effective collection time of fluorescence per single protein molecule is therefore ≅ 360 μs. Molecules were not irradiated during the remaining image acquisition. Fields of view with only 5–30 fluorescence spots that correspond to single GFPmut2 molecules (Chirico et al. 2001; Cannone et al. 2005b) were selected. For good statistics about 600 single molecules were examined. In control experiments, fluorescence intensity as a function of time was recorded on selected single molecules.

Results and discussion

The main aim of this study is to follow the denaturation *kinetics* of single GFP-mut2 proteins in silica gel in a wide range of denaturant concentrations in order to point out possible multi-step unfolding pathways or unfolding–refolding competition. Denaturation has been induced by raising the GuHCl concentration in wet silica gels loaded with GFP-mut2 proteins.

Experimental background

A set of preliminary control experiments have been performed and reported previously (Cannone et al. 2005a). In summary, (1) GFPmut2, when excited at ≅ 840 nm, emits on the green (≅ 510 nm) and the blue (≅ 460 nm) channels that can be ascribed to the emission of the anionic and neutral form of the chromophore. (2) Changes in the secondary structure have been followed by CD experiments in bulk solutions and gels and found to correlate well with the change of the fluorescence signal in the same conditions on single proteins (Cannone et al. 2005a; Campanini et al. 2005). (3) The unfolding rate estimated from the decay of the

number of fluorescent molecules versus time after the addition of the denaturant to the gel is in good agreement with the measurements performed on bulk protein samples in gels (Cannone et al. 2005a; Campanini et al. 2005). (4) The denaturant diffusion through the gel pores occur in the first 1–2 s from the addition of the denaturant to the gel (Cannone et al. 2005a). All the denaturation relaxation times are of the order of tens of minutes, therefore unaffected by this delay time. (5) Fluorescence bleaching can be induced by raising the excitation intensity and/or the image sampling frequency (i.e., the residence time on the single molecule), and by the addition of denaturant agents to the gels. We have shown previously (Cannone et al. 2005a; Campanini et al. 2005) that irradiation below 2 MW/cm^2 and single molecule illumination frequency below ≅ 1/900 Hz ensures that no photobleaching is occurring: the number of the fluorescent proteins observed on a field of view is stable for ≅ 10 h. In this regime the action of the denaturant agent alone can be followed. (6) A two-state model can fit the fraction of unfolded proteins versus the denaturant concentration (Cannone et al. 2005a). (7) For refolding, single proteins recover fluorescence emission with a fast (< 15 min) process and with a perturbed population ratio of the neutral and anionic state. The equilibrium population ratio observed before unfolding is reached after refolding with a slow relaxation (relaxation time ≅ 60–70 min) (Cannone et al. 2005a).

Single protein unfolding

The number of single fluorescent proteins in a field of view decreases with time (a movie of the unfolding kinetics is available in ''avi'' format). By plotting the number of fluorescent proteins observed on either the anionic or the neutral channel versus time, we observe decays (plot in Fig. 1) from a value N_0 at $t = 0$ (defined as the time at which the gel has been loaded with GuHCl) to an equilibrium value N_∞ reached after ≅ 50–200 min, depending on [GuHCl]. The decays observed on the two channels are very similar in terms of shape and average relaxation rates, although the recovery of the proteins on the two channels upon refolding is different as described in detail elsewhere (Cannone et al. 2005a). The simultaneous detection of the neutral and anionic channels is essential to avoid to take fluorescence blinking as a fluctuation in the number of folded proteins. Although the emission filter bands (515 ± 20 and 460 ± 20) cover most of the emission spectrum of the GFP mutant, we cannot rule out the possibility that other intermediate states exist, with slightly distinct spectral properties.

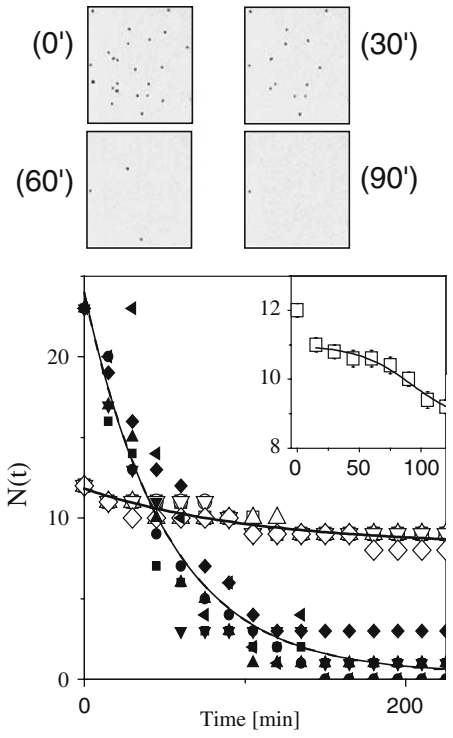

Fig. 1 Images: a 10 × 10 μm field of view of silica gel at various time delay from the GuHCl addition (4.45 M) to the gel. The spots correspond to single GFP molecules emitting in the anionic channel only. The *numbers* in the *round parentheses* are minutes from the addition of the denaturant. *Main panel*: number of fluorescent (on either A or B channel) molecules versus time after the addition of GdHCl to the gel. *Different symbols* refer to different fields of view. *Filled* and *open symbols* refer to [GdHCl] = 4.45 and 0.45 M, respectively. *Solid lines* are global single exponential fit to the data at each denaturant concentration. Best fit decay rates are $\gamma_U = 0.2$ min^{-1}, $N_\infty = 8.5 \pm 0.4$, $N_0 = 11.9 \pm 0.4$ and $\gamma_U = 0.01$ min^{-1}, for 4.45 and 0.45 M, respectively. *Inset*: average of the $N(t)$ decay for 0.45 M GuHCl. *Dashed line* is the best fit according to Eq. 12 in the text

It must be noted that at equilibrium a defined number of proteins, determined by the GuHCl concentration, are in the unfolded/dark state. The fluorescence recovery at some spots in the field of view would imply that unfolded (i.e., non-fluorescent) proteins could recover, at least partially, the folded conformation, in agreement with the dynamic equilibrium that is expected for a two-state chemical reaction. Unexpectedly, we have observed over a sample of ≅ 200 molecules only rare events of unfolded GFP proteins that temporarily recover fluorescence emission, i.e., refold, with an estimated rate of ≅ 0.004 min^{-1}. The fluorescence recover of single GFP proteins is even more rare during the unfolding process. From Fig. 1 it is evident that the number decay of the fluorescent proteins is mainly monotonic, and we observe only very few events of recovery of fluorescence from previously unfolded proteins. The low rate of spontaneous

refolding recovery is detected also below the midpoint concentration and prevent a reliable direct estimate of the refolding rate, k_f, from unfolding experiments. Nevertheless both unfolding and refolding processes affect the overall measured unfolding kinetics even in single molecule experiments, as can be seen from the following analysis.

Two features are evident in the number decays: a fast decay with relaxation times < 15 min and a systematic roll-off at small lag times and at low [GuHCl] (inset of the plot in Fig. 1). The fast decay component, confirmed by the acquisition of the fluorescence signal of single proteins at high time resolution (100 μs) and lower excitation intensities (50 kW/cm^2), indicates a population of GFP molecules that looses fluorescence emission within the first 2–4 s, *after* that the denaturant has diffused through the gel (which occurs in 1–2 s) (Cannone et al. 2005a). This fast decay, observed also in bulk gels and solutions, is compatible with the $N(t)$ relaxation time < 15 min measured when adding NaCl alone to the protein-loaded silica gels (data not shown), and therefore is probably due to an aspecific chemical effect of NaCl on the quantum yield of the GFP chromophore. NaCl might generate a landscape for the protein, different from that induced by GuHCl which should be effective only over larger lag times.

The systematic roll-off at small lag times visible at low [GuHCl] (inset of the plot in Fig. 1, solid line) is not reproduced in data collected at high [GuHCl]. Apart from these features, we can describe the number decay by means of a single exponential function:

$$N(t) = (N_0 - N_\infty)e^{-\gamma_U t} + N_\infty \quad (1)$$

in the whole range of [GuHCl] explored, 0.45–4.45 M. The decay rate γ_U increases as a function of denaturant concentration and we expect that $\gamma_U = k_u + k_f \cong k_u$ is mostly determined by the relaxation rate for unfolding equilibrium, since we are performing denaturation experiments.

Single protein unfolding time distribution

Since the refolding rate cannot be directly estimated from single molecule data, we come to analyze the shape of the $N(t)$ decays. Actually, the $N(t)$ decays measured on the fields of view of limited size are affected by a relevant statistical uncertainty. It is therefore difficult to assess whether a single exponential function reliably describes the decay. An alternative characterization of the shape of the $N(t)$ decays versus time can be made by evaluating the probability of finding proteins with a given unfolding time, τ_U. In a simple two step unfolding process, the probability $P(\tau_U)$ of finding a single protein with unfolding time τ_U is related to the number of fluorescent molecules at time τ_U as:

$$P(\tau_U) = -\frac{(k_u + k_f)}{k_u N_0}\frac{dN(t)}{dt}\bigg|_{t=\tau_U} \quad (2)$$

k_u, k_f are the folding and unfolding relaxation rates *at the denaturant concentration in the system*, and N_0 is the number of fluorescent molecules observed just before the addition of denaturant, $N(t = 0)$. Although the unfolding probability could be determined from the first time derivative of the number of observed fluorescent molecules, more direct methods should be preferred as done here. The experimental $P(\tau_U)$ functions are plotted versus τ_U in Fig. 2 for different concentrations of GuHCl.

The component observed at τ_U = 15 min (≅ 30% in amplitude) in $P(\tau_U)$ corresponds to the fast decay observed in bulk gels both in fluorescence (inset in the plot of Fig. 1) and CD spectroscopy (Campanini et al. 2005) that is ascribed to an *aspecific effect* of NaCl on the protein quantum yield. The striking feature of $P(\tau_U)$ is that, for [GuHCl] < 3.5 M, a well-defined peak is found for $\tau_U \cong 1/\gamma_U$.

The maximum observed in the unfolding time distributions for GuHCl might be described by a two-step transition of the type:

$$E \leftrightarrow D \leftrightarrow C \quad (3)$$

where C is the unfolded (dark) state and the unfolding occurs from an intermediate bright D state. The $D \rightarrow C$ and the $E \rightarrow D$ steps would be the fast and the rate limiting process, respectively. A fast fluorescence bleaching upon raising the GuHCl concentration, would correspond to the unfolding of the molecules already in the D state, i.e., the $D \rightarrow C$ transition. After the D state is depleted, a time lag is needed to populate it back according to the slower transition $E \rightarrow D$. This model is attractive. However, some observations prevent $P(\tau_U)$ to be quantitatively described in this way. First, the observed fast decay ($\tau_U \cong 15$ min) cannot account for the $D \rightarrow C$ transition as in the above model, since it is more likely ascribed to an aspecific NaCl effect. Second, the experiments show no evidence of two fluorescent species (E and D) at [GuHCl] = 0 M, neither in terms of molecular brightness nor of the excited state fluorescence lifetimes. Third, the kinetics of any of the three states in a two-step model is given by a sum of *only* two exponential decays:

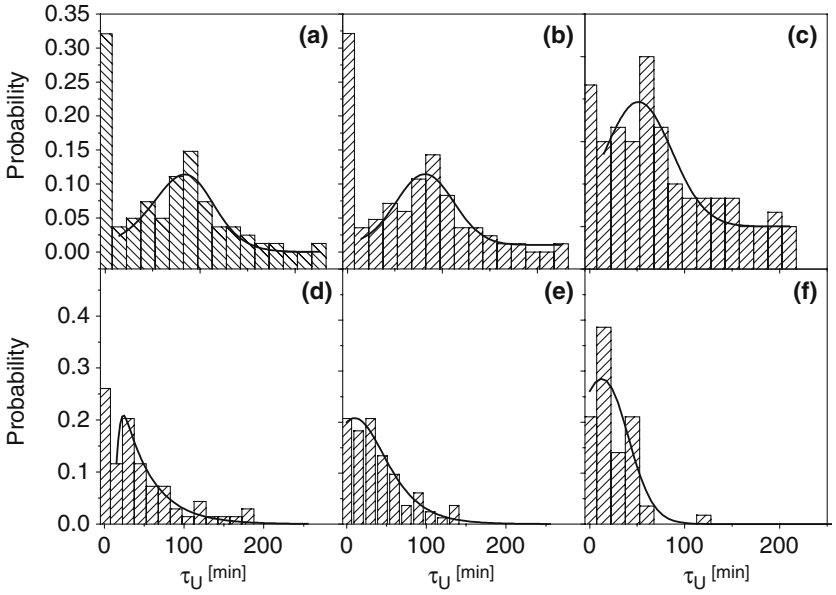

Fig. 2 Probabilities of finding bleaching time τ_U induced by the addition of GuHCl. Concentrations [GuHCl] are: 0.45 M (**a**), 1.45 M (**b**), 2.45 M (**c**), 3.45 M (**d**), 4.45 M (**e**), 5.0 M (**f**). *Solid lines* are best fit to the data according to the competition model presented in the text (Eq. 11). The first bin of the distributions have not been taken into account in the fit (see text)

$$X = X_0 + X_p \exp\left(-t\lambda_p\right) + X_m \exp\left(-t\lambda_m\right) \quad (4)$$

where $X = C$, D or E. The relaxation rates λ_p and λ_m (assumed $\lambda_p > \lambda_m$) are related to the forward and backward kinetics rate of the two steps in the reaction and are *the same for all the three states*, C, D, and E. In the above model, we expect that $D_p < 0$ while $D_m > 0$ and E_p, $E_m > 0$. Typical trends for the D and E populations are shown in Fig. 3. In general, the condition $\left.\frac{dN(t)}{dt}\right|_{t=0} = -P(t=0) \cong 0$ is not compatible (see Appendix 1) with the requirement that the unfolding time distribution is a positive defined function, $\left.\frac{dN(t)}{dt}\right|_{t} = -P(t) > 0$ for $t > 0$, and with the requirement that $P(t)$ shows a maximum for some unfolding time $\tau_U > 0$.

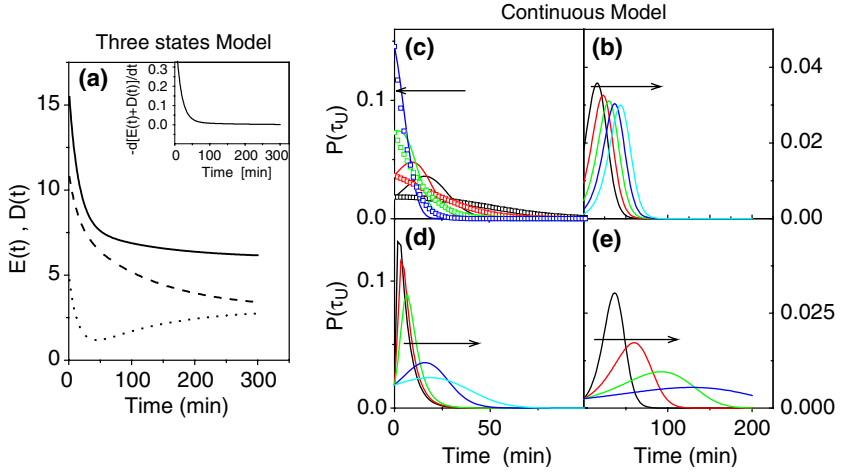

Fig. 3 **a** Three states model: simulations of the decay of the number of proteins in the folded states according to the three states unfolding model, $E \leftrightarrow D \leftrightarrow C$. The *dashed* ($E$ species) and *dotted* (D species) *lines* are computed according to $X = X_0 + X_p \exp(-t\lambda_p) + X_m \exp(-t\lambda_m)$ for $X = E$ or D: $E_0 = E_p = 3$, $E_m = 5$ and $D_0 = 3$, $D_p = 5$, $D_m = -3$. For both the decays $\lambda_p = 15$ min and $\lambda_m = 120$ min. The *solid line* represents the sum of the D and E decays. *Inset*: opposite of the first derivative of the number of molecules that is proportional to the single molecule unfolding time distribution $P(\tau_C)$. *Right panel* (continuous model): simulations made according to Eq. 11 (see text). **b** $\lambda_\infty = 0.3$; $\tau_0 = 10$; $\delta = 10$ (*black*), 20 (*red*), 40 (*green*), 80 (*blue*), 160 (*cyano*). **c** *Solid lines*, $\tau_0 = 10$; $\delta = 10$; $\lambda_\infty = 0.2$ (*black*), 0.4 (*red*), 0.8 (*green*), 1.6 (*blue*). *Open Squares* $\tau_0 = 50$; $\delta = 10$; $\lambda_\infty = 0.2$ (*black*), 0.4 (*red*), 0.8 (*green*), 1.6 (*blue*). **d** $\lambda_\infty = 0.2$; $\delta = 10$; $\tau_0 = 0.5$ (*black*), 1 (*red*), 2 (*green*), 10 (*blue*), 20 (*cyano*). **e** $\lambda_\infty = 0.2$; $\delta = 80$; $\tau_0 = 10$ (*black*), 20 (*red*), 40 (*green*), 80 (*blue*)

Unfolding–refolding competition model

A three-step model would probably account reasonably well for the observed shape of $N(t)$ and $P(\tau_U)$. However, before assuming a more complex model, one should consider what is the effect of the competition between the unfolding and the refolding processes in the observed $N(t)$ decay and what are the experimental conditions of single molecule experiments. The basic equation for the two-state model is summarized as:

$$\begin{cases} \frac{dN}{dt} = -k_u N(t) + k_f U(t) \\ N(t) + U(t) = M \end{cases} \quad (5)$$

where $N(t)$ and $U(t)$ are the time dependent number of proteins in the native and unfolded states and M indicates the total number of proteins. The formal solution of this equation is given by:

$$N(t) = \frac{M}{\lambda}\{k_f + k_u \exp[-\lambda t]\} \quad (6)$$

where $\lambda = k_f + k_u$. A crucial and apparently obvious step in this derivation is that $U(t) = M–N(t)$. However, when observing single protein unfolding, statistical effects become relevant. In fact, unfolding experiments performed on single molecules correspond to: $[GuHCl]|_{t=0} = 0 \left| ; \frac{d[GuHCl]}{dt}\right|_{t=0} > 0$, $N(0) = M$ and $U(0) = M–N(0) = 0$. In bulk samples M is large and a small but finite contribution from the unfolded population is always present, due to thermodynamic equilibrium. On the contrary, in single molecule experiments, it is likely that $U(0)$ is identically null for a appreciable stretch of time after the beginning of unfolding. Therefore, k_f plays no role at all in this first unfolding regime (Eq. 5) under single molecule conditions. The first of Eq. 5 reads then for $t \cong 0$ approximately:

$$\frac{dN}{dt} \cong -k_u N(t) \quad (\text{unfolding experiment},\ t \cong 0) \quad (7)$$

even at low denaturant concentration, for which $k_u \ll k_f$, since $U(0) = 0$. The solution of Eq. 7 is a single exponential with decay rate = k_u. After some time from the addition of the denaturant, the number of unfolded proteins raises and also k_f plays a role (see Eq. 6) in the unfolding kinetics, and the folded protein number decays according to the rate $\lambda = k_f + k_u$, as expected in bulk experiments. Therefore, the behavior described here can be modeled, in a first approximation, as an unfolding process in which the folding/unfolding rates are time-dependent (see Appendix 1 and 2): from k_u for $t \cong 0$ to λ for $t \geq 1/\gamma u$. It must also be noted that the observed roll-off in the number decay at small denaturant concentration is a signature of the behavior just described that is clearly more effective around the denaturation midpoint where the unfolding kinetics is slower.

When we consider the refolding experiments the conditions are $[GuHCl]|_{t=0} \gg 0; \frac{d[GuHCl]}{dt}\Big|_{t=0}$ and $N(0) = 0$ while $U(0) = M$. The first of Eq. 5 reads then for $t \cong 0$ approximately:

$$\frac{dN}{dt} \cong -k_f(M - N(t)) \quad (\text{refolding experiment},\ t \cong 0) \quad (8)$$

even at high denaturant concentration, for which $k_u \gg k_f$, since $N(0) = 0$.

An unfolding experiment will provide an accurate estimate of the unfolding rate only, and the refolding rate should be determined from a refolding experiment (Matouschek et al. 1990). However, Eqs. 7 and 8 are valid for $t \cong 0$ only. When the unfolding or the refolding process is taking place in conditions far from the transition midpoint $[GUHCl]_{0.5}$, the competitor process (refolding or unfolding) is becoming effective (i.e., the terms $k_u N(t)$ and $k_f U(t)$ become comparable in Eq. 5 for $t \to \infty$), leading to a non-exponential behavior of the number decay. It must be noted again that this behavior is intrinsically due to the statistical effects in single molecule observations. In a bulk experiment, even in the very first time regime, both k_f and k_u play a role, determining together the exponential trend of $N(t)$ according to Eq. 6.

How can we try to model such a behavior? As said above, one possibility is to assume that the rates in Eq. 2 are time dependent: the unfolding process is passing through a series of two-state unfolding situations where the unfolding rate is changing with time.

In this case (see Appendix 2) the unfolding time probability distribution, $P(\tau_U)$, and the number of folded proteins, $N(t)$ are related by the equation:

$$P(t) = -\frac{\lambda(t)}{k_u(t)N_0}\frac{dN}{dt} \quad (9)$$

where $k_u(t)$, $k_f(t)$ and λ (t) are the folding, unfolding and the total relaxation rates and $N_0 \cong M$ is the number of fluorescent molecules observed just before the addition of denaturant. The exact shape of the time dependence of the relaxation rates should be derived from the reasoning given above. However, for the sake of simplicity, we assume in the following that the functional dependence of λ (t) and $k_f(t)$ can be described (see Appendix 2) as:

$$\lambda(t) = \frac{\lambda_\infty}{1+\delta\exp(-t/\tau_0)}$$
$$k_u(t) = \frac{k_\infty}{1+\delta\exp(-t/\tau_0)} \quad (10)$$

where k_∞ and λ_∞ are the limiting values of the unfolding and the total relaxation rates for $t \to \infty$. The characteristic time τ_0 is related to how fast the less represented component (U in unfolding experiments) increases, and therefore to k_f. The parameter δ is such that: $\lambda(t = 0) = \lambda_\infty/(1 + \delta)$ and $\lambda(t \to \infty) = \lambda_\infty$. When performing unfolding experiments well above the midpoint denaturation concentration $[GuHCl]_{0.5}$, $\lambda(t = 0) \cong \lambda_\infty \cong k_u$ and $\delta \cong 0$. On the other hand, when performing unfolding experiments well below the midpoint denaturation concentration $[GuHCl]_{0.5}$, $\lambda(t = 0) \cong k_u$ while λ_∞ should be determined both by k_f and k_u. In these conditions $\delta \gg 0$, since $k_u \ll k_f$.

The probability function for the unfolding times, τ_U, derived from Eqs. 9, 10 and Eq. 17, has the form:

$$P(\tau_U) = \lambda(\tau_U)\left(\frac{1+\delta}{1+\delta\exp[-\tau_U/\tau_0]}\right)^{\tau_0\lambda_\infty}\exp[-\lambda_\infty\tau_U]. \quad (11)$$

An analysis of Eq. 10 shows that: (1) $P(\tau_U)$ displays a maximum for $\tau^{max}_U = \tau_0 \ln(\delta/\tau_0\lambda_\infty)$; (2) $P(\tau_U)$ becomes exponential $\cong \lambda_\infty \exp[-\lambda_\infty\tau_U]$, in the limit $\delta \to 0$; (3) $P(\tau_U)$ approaches again a single exponential decay for $\tau_0\lambda_\infty \gg 1$, with a decay rate $\lambda_\infty/(1 + \delta)$.

The functional form of $P(\tau_U)$ leads also to write the number of single fluorescent (i.e., folded) molecule at time t as:

$$N(t) = (N_0 - \langle N\rangle_\infty)\left(\frac{1+\delta}{1+\delta\exp[-t/\tau_0]}\right)^{\tau_0\lambda_\infty} \times \exp[-\lambda_\infty t] + \langle N\rangle_\infty \quad (12)$$

where $\langle N\rangle_\infty = N_0\, k_{f\infty}/\lambda_\infty$. The time behavior of the number of molecules is close to an exponential decay with a reduced first derivative at $t = 0$ with respect to the exponential trend. This behavior is indeed found in the experimental curves, $N(t)$, at low GuHCl concentration (Fig. 1, inset). Again for $\delta \to 0$ the decay is well approximated by a simple exponential function, $(N_0 - \langle N\rangle_\infty)\exp[-\lambda_\infty t] + \langle N\rangle_\infty$.

Numerical simulations of the competition model

We will first assess if the unfolding time distributions measured for GuHCl (Fig. 2) can be described by Eq. 11 for $\tau_U > 15$ min. Simulations reported in Fig. 3 indicate that a maximum occurs in $P(\tau)$ at $\tau^{max} \cong \tau_0 \ln(\delta/\tau_0\lambda_\infty)$, as expected. No evidence of a maximum in $P(\tau_U)$ can be found when the product $\lambda_\infty\tau_0 \gg 10$ and its shape approaches an exponential function (Fig. 3c). However, the decay rate of $P(\tau)$ is $\cong \lambda_\infty/(1 + \delta)$, lower than λ_∞. On the other hand, when $\tau_0\lambda_\infty \ll 1$, one obtains an exponential decay that is well described by the function $\lambda_\infty\exp[-\lambda_\infty\tau_U]$ (see Fig. 3d). Finally, we notice that the role of the steepness, δ, of the unfolding rate function, $\lambda(\tau)$ is to enhance the non-exponential behavior of $P(\tau)$. In fact, as δ increases, the maximum of the $P(\tau)$ distribution shifts toward larger values of τ_U (Fig. 3b).

We now turn to compare the shape of the experimental to the simulated distributions, $P(\tau_U)$. The maximum of the distributions found for the case of GuHCl (Fig. 2), moves towards smaller values of τ_U as the denaturant concentration increases, while the width of the distribution does not seem to be largely affected. From Fig. 3b, e one can see that both a reduction of τ_0 and of δ causes a shift of the maximum of the $P(\tau_U)$ distribution toward smaller values of τ_U. However, δ does not affect the width of the distribution, which is mostly determined by the value of τ_0 (see Fig. 3e). We expect then to obtain fairly constant values of τ_0 from the fit of the experimental distributions at least for [GuHCl] < 3.5 M, where the maximum in the distribution is clearly discernible. The results of the best fit of $P(\tau_U)$ are reported in Table 1. The best fit relaxation time τ_0 is $\tau_0 = 25 \pm 5$ min and should be related to the refolding rate, k_f. The value of τ_0 is about 1/4 of the average unfolding time $1/\gamma_U \cong 100$ min (see Table 1), in agreement with the observation that the refolding occurs on a faster time scale ($\cong 15$ min) than unfolding (Cannone et al. 2005b). On the contrary, the parameter δ decreases with the denaturant concentration from $\cong 50$ to about 1. The best fit values of λ_∞ are in the range 0.04–0.07 min^{-1}, and correspond to $\tau_0\lambda_\infty \cong 1$–1.75.

Finally we notice that the continuous unfolding model set here for the τ_U distributions also gives a consistent description of the number decays, $N(t)$. As an example, we show in Fig. 4 the fit of the $N(t)$ decays measured for 0.45 and 4.45 M GuHCl, to the theoretical prediction given by Eq. 12. At low [GuHCl] the non-exponential decay behavior seems slightly more evident, as can be judged by the comparison of the single exponential fit to that obtained from Eq. 12. However, this is probably due only to the statistical uncertainty related to the small number of proteins observed in the field of view. We also notice that the number relaxation rate γ_U at low denaturant concentration is approximately five- to seven times lower

Table 1 Best fit values of the number decays and unfolding time distributions

[GuHCl] (M)	5.0	4.45	3.45	2.45	1.45	0.45
λ_∞ (min^{-1})	0.065 ± 0.01	0.049 ± 0.01	0.039 ± 0.02	0.049 ± 0.04	0.075 ± 0.02	0.07 ± 0.02
τ_0 (min)	25[a]	25[a]	26 ± 12	23 ± 10	26 ± 7	25 ± 9
δ	1 ± 0.5	1.9 ± 0.9	2.6 ± 2	11 ± 7	51 ± 30	48 ± 30
γ_P (min^{-1})	0.04 ± 0.004	0.013 ± 0.003	0.013 ± 0.01	–	–	–
γ_U (min^{-1})	–	0.019 ± 0.002	–	0.012 ± 0.002	–	0.01 ± 0.002

Best fit parameters of the distribution of denaturation times measured upon GuHCl addition according to the model discussed in the text. γ_P is obtained from the single exponential fit to the $P(\tau_U)$ distributions. γ_U is obtained from the single exponential fit to the $N(t)$ decays

[a]The value $\tau_0 = 25$ min has been assumed for fitting unfolding time distributions at these concentrations

than λ_∞, probably due to the round-off at low τ_U times in the $N(t)$ decays.

Conclusions

We have observed extremely low rates of spontaneous transitions between unfolded/dark and folded/bright conformation of single GFP protein at equilibrium. Moreover, in unfolding experiments, the relaxation time distribution of single GFP-mut2 proteins shows a non-exponential behavior, at [GuHCl] $\ll$ [GuHCl]$_{0.5}$. This trend can be analyzed according to a simplified theoretical treatment that suggests an interplay and competition of the unfolding and refolding processes, whose effect is mostly visible in the unfolding time distribution as measured from single molecule experiments. The treatment given here suggests therefore that single molecule spectroscopy data could help in discriminating both unfolding and refolding rates in either an unfolding or refolding experiment. As a matter of fact, the unfolding relaxation rate determined here by the unfolding time distribution analysis has a marked linear trend over almost the full range of denaturant concentration explored (Fig. 5) contrary to what found when measuring the single exponential rate of the native protein number $N(t)$.

It is worth noting that the evaluation of the unfolding rate on the whole range of denaturant concentration described above could not be obtained also from an analysis of the first derivative of the bulk fluorescence measurements, due to statistical reasons related to the finite size of the molecular ensembles monitored by single molecule experiments. Moreover,

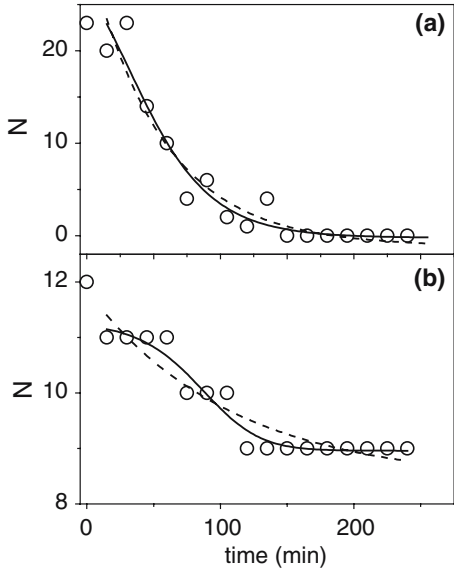

Fig. 4 Decay of the number of fluorescent proteins, $N(t)$, for [GUHCl] = 4.45 M (**a**) and 0.45 M (**b**). Superimposed to the data are shown the best fit curves according to a single exponential function $\cong \exp(-\tau\gamma_U)$ (*dashed lines*) and to Eq. 12 (*solid lines*). The parameters for the case [GuHCl] = 4.45 M are, (*solid line*) $N_0 = 26$, $\tau_0 = 25$ min, $\lambda_\infty = 0.029$ min^{-1}, $\delta \cong 2.6$ and (*dashed line*) $\gamma_U \cong 0.018 \pm 0.004$ min. For the case [GuHCl] = 0.45 M the parameters are: (*solid line*) $N_0 = 11$, $N_\infty = 9$, $\tau_0 = 26$ min, $\lambda_\infty = 0.063$ min^{-1}, $\delta \cong 48$, and (*dashed line*) $\gamma_U \cong 0.0093 \pm 0.0012$ min

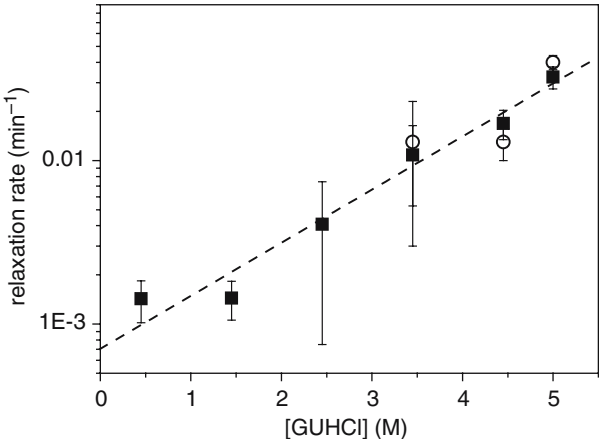

Fig. 5 Unfolding relaxation rates obtained by means of the unfolding time distribution analysis discussed in the text. *Filled squares* refer to the values $\lambda\ (t = 0) = \lambda_\infty/(1 + \delta)$. *Open circles* refer to the relaxation rates of the protein number decay, γ_U. The data are reported in Table 1. The *solid line* is a linear fit to the whole set of data plotted

the extremely low rate of spontaneous exchange between native and unfolded conformations could be determined from single molecule experiments only. We can also speculate on the extremely low rate of exchange between unfolded/dark and folded/bright conformations of single GFP proteins observed here. The estimate of the refolding rate at denaturant concentration below the denaturation midpoint is far too low than what expected, since, in this condition the refolding rate should be larger than the unfolding one. In a simple two-step transition the kinetics are determined by the energy barriers between the two states. In equilibrium conditions at very high or low denaturant concentrations, one of the two energy barriers dominates and very low probability of exchange is indeed expected. However, close to the midpoint denaturation concentration, the energy barriers for the back and forward reactions are very similar and a maximum of the folded/unfolded exchange rate is expected. The observations reported here might suggest that unfolding and refolding are multiple steps processes in which several energy barriers must be overcome to exchange from folded to unfolded conformation and vice versa.

Finally it must be noted that the theoretical model discussed here could be applied to highly confined or constrained protein systems where, indeed, the unfolding or refolding rates could be time dependent due to a slow protein conformational rearrangement or protein–denaturant interaction.

Acknowledgements The research reported in this work has been funded by a PRIN grant of the Ministry of Research and Education of Italy to G.C. and A.D. for the years 2004–2005. The financial support of FIRB Nanotechnology 2003 and of FISR (MIUR) is also gratefully acknowledged. We are grateful to Andrea Mozzarelli and Stefano Bettati for their useful discussions and to Barbara Campanini for her help in the silica gel preparation.

Appendix 1: positive defined unfolding distribution

Let us take a general two exponential decay with a background that can be used to fit the fluorescent molecules number $N(t)$ decay:

$$X(t) = X_0 + X_p \exp\left(-t\lambda_p\right) + X_m \exp\left(-t\lambda_m\right). \tag{13}$$

The opposite of the derivative of this function is the unfolding time distribution. In order to describe both the number decay (a monotonically decreasing function) and the unfolding time distribution ($P(t = 0) \cong 0$ and $P(t = \tau_U) \cong 0$ and $P(t) > 0$ otherwise) we must fulfill the following requirements:

$$\begin{cases} X_0 + X_p + X_m > 0 \\ \lambda_p X_p + \lambda_m X_m \cong 0 \\ \lambda_p X_p \exp\left[-\lambda_p t\right] + \lambda_m X_m \exp\left[-\lambda_m t\right]\big|_{t>0} \geqslant 0 \end{cases} \tag{14}$$

These conditions can be cast as

$$\begin{cases} X_0 > X_p \left[\frac{\lambda_p}{\lambda_m} - 1\right] \\ X_m \cong -\frac{\lambda_p X_p}{\lambda_m} \\ -\lambda_p X_p \left\{\exp\left[-\lambda_p t\right] - \exp\left[-\lambda_m t\right]\right\}\big|_{t>0} \geqslant 0 \end{cases} \tag{15}$$

However, the last of the equations (Eq. 15) could be fulfilled only for $t = 0$. For any value $t > 0$, this expression is negative and this would correspond to the unphysical result that the unfolding time distribution is negative and no other maximum in the unfolding time distribution is found, contrary to the experimental evidence.

Appendix 2: retarded unfolding

In the standard stopped-flow experiment the kinetics of the number of native $N(t)$ and unfolded $U(t)$ proteins fluctuate in time around an equilibrium value $\langle N \rangle_0$ and $\langle U \rangle_0$ according to the unfolding and folding rates, $k_{u,0}$, $k_{f,0}$ as:

$$\frac{dN(t)}{dt} = -k_{u,0}N(t) + k_{f,0}U(t). \tag{16}$$

Let us suppose here that the initial number of native proteins is N_0. If we induce a sudden increase in the concentration of a chemical denaturant, such as GuHCl, at time $t = 0$, the protein system is then brought out of the equilibrium condition and the new equilibrium value of the native proteins is $\langle N \rangle$. Also the kinetics rates will reach different values, k_f and k_u, *in a time that is much smaller than the characteristic time of the relaxation kinetics* $\cong (k_{f0} + k_{u0})^{-1}$. The number of fluorescent molecules $N(t)$ and the probability of measuring a value τ_U of the unfolding time $P(\tau_U)$ are related in general by:

$$N(t) = \frac{\langle N \rangle}{k_f}\left(\lambda - k_u \int_0^t P(x)dx\right) \tag{17}$$

where $\lambda = k_u + k_f$ and $\langle N \rangle = N_0\, k_f/\lambda$. Eqs. 16 and 17 lead to the exponential decay of the number of native molecules and to the exponential shape of the probability $P(\tau_U)$. Eq. 17 ensures that the distribution function $P(\tau_U)$ is normalized.

However, if the kinetics rates change in a time that is comparable with the relaxation time of the protein system, then $\langle N \rangle$, k_f, k_u and λ will be the function of time and the integral relation between $N(t)$ and $P(\tau_U)$ can be cast as

$$P(t) = -\frac{\lambda(t)}{k_u(t)N_0}\frac{dN}{dt} - \left[\frac{d}{dt}\ln\left(\frac{k_u}{\lambda}\right)\right]\int_0^t P(x)dx. \qquad (18)$$

This equation is not easily treated unless we make the assumption that the time change of the relaxation rates is similar so that the term that multiplies the integral at the right-hand term of the equation vanishes, leading to the more treatable equation:

$$P(t) = -\frac{\lambda(t)}{k_u(t)N_0}\frac{dN}{dt}. \qquad (19)$$

Now, the time behavior of the relaxation rates should be related to a change of the activation energies, $\Delta G_f^{0\#}$=*ln* (k_f) and $\Delta G_u^{0\#}$=*ln* (k_u). For a two-state model we may assume a behavior of the type:

$$\Delta G_f^{0\#}(t) = KT(\beta + \gamma \exp[-t/\alpha]). \qquad (20)$$

In this case the relaxation rates $k(t) = \exp[-\Delta G^{0\#}(t)/KT]$ can be well approximated by a sigmoidal function with a mid-time $\cong \alpha \ln(\gamma)$. We can than assume that the functional dependence of λ(t) and k_f(t) is:

$$\begin{aligned}\lambda(t) &= \frac{\lambda_\infty}{1+\delta\exp(-t/\tau)} \\ k_u(t) &= \frac{k_\infty}{1+\delta\exp(-t/\tau)}\end{aligned}. \qquad (21)$$

With this functional dependence, the assumption that $\frac{d}{dt}\ln\left(\frac{k_u}{\lambda}\right) = 0$ in Eq. 18 is implicitly satisfied. The probability function for the bleaching times has then the shape:

$$P(t) = \lambda(t)\left(\frac{1+\delta}{1+\delta\exp[-t/\tau]}\right)^{\tau\lambda_\infty}\exp[-\lambda_\infty t]. \qquad (22)$$

The relaxation time that we could measure in a usual stopped-flow denaturation experiment is λ_∞. The shape of $P(\tau_U)$ becomes exponential in the limit $\tau \to 0$ as expected.

On the other hand, the number that can be derived from Eqs. 16 and 17 is:

$$N(t) = (N_0 - \langle N\rangle_\infty)\left(\frac{1+\delta}{1+\delta\exp[-t/\tau]}\right)^{\tau\lambda_\infty} \times \exp[-\lambda_\infty t] + \langle N\rangle_\infty, \qquad (23)$$

where $\langle N \rangle_\infty = N(0)\, k_{f\infty}/\lambda_\infty$.

The time behavior of the number of molecules is then close to an exponential decay but it shows a reduced first derivative at $t = 0$ with respect to the exponential trend.

References

Badjic JD, Kostic NM (1999) Effects of encapsulation in sol-gel silica glass on esterase activity, conformational stability, and unfolding of bovine carbonic anhydrase II. Chem Mat 11:3671–3679

Baldini G, Cannone F, Chirico G (2005) Pre-unfolding resonant oscillations of single green fluorescent protein molecules. Science 309:1096–1100

Bettati S, Mozzarelli A (1997) T state hemoglobin binds oxygen noncooperatively with allosteric effects of protons, inositol hexaphosphate and chloride. J Biol Chem 272:32050–32055

Campanini B, Bologna S, Cannone F, Chirico G, Mozzarelli A, Bettati S (2005) Unfolding of green fluorescent protein mut2 in wet nanoporous silica gels. Protein Sci 14:1125–1133

Cannone F, Chirico G, Baldini G, Diaspro A (2003) Measurement of the laser pulse width on the microscope objective plane by modulated autocorrelation method. J Microsc 210:149–157

Cannone F, Bologna S, Campanini B, Diaspro A, Bettati S, Mozzarelli A, Chirico G (2005a) Tracking unfolding and refolding of single GFPmut2 molecules. Biophys J 89:2033–2045

Cannone F, Caccia M, Bologna S, Diaspro A, Chirico G (2005b) Single molecule spectroscopic characterization of GFP-MUT2 mutant for two-photon microscopy applications. Microsc Res Tech 65:186–193

Chirico G, Cannone F, Beretta S, Baldini G, Diaspro A (2001) Single molecules studies by means of the two-photon fluorescence distribution. Microsc Res Tech 55:359–364

Chirico G, Cannone F, Beretta S, Diaspro A, Campanini B, Bettati S, Ruotolo R, Mozzarelli A (2002) Dynamics of green fluorescent protein mutant2 in solution, on spin-coated glasses and encapsulated in nanoporous silica gels. Protein Sci 11:1152–1161

Cormack BC, Valdivia RH, Falkow S (1996) FACS-optimized mutants of green fluorescent protein (GFP). Gene 173:33–38

Diaspro A (2001) Building a two-photon microscope using a confocal laser scanning architecture. In: Periasamy A (ed) Methods in cellular imaging. Oxford University Press, New York, pp 162–179

Dill KA, Chan HS (1997) From Levinthal to pathways to funnels. Nat Struct Biol 4:10–9

Eaton WA, Munoz V, Hagen SJ, Jas GS, Lapidus LJ, Henry ER, Hofrichter J (2000) Fast kinetics and mechanisms in protein folding. Annu Rev Biophys Biomol Struct 29:327–359

Ellerby LM, Nishida CR, Nishida F, Yamanaka SA, Dunn B, Valentine JS, Zink JI (1992) Encapsulation of proteins in transparent porous silicate glasses prepared by the sol-gel method. Science 28:1113–1115

Jackson SE, Fersht AR (1991) Contribution of long-range electrostatic interactions to the stabilization of the catalytic transition state of the serine protease subtilisin BPN'. Biochemistry 30:10428–10435

Kubelka J, Hofrichter J, Eaton WA (2004) The protein folding 'speed limit'. Curr Opin Struct Biol 14:76–88

Lindorff-Larsen K, Rogen P, Paci E, Vendruscolo M, Dobson CM (2005) Protein folding and the organization of the protein topology universe. Trends Biochem Sci 30:13–19

Lipman EA, Schuler B, Bakajin O, Eaton WA (2003) Single-molecule measurement of protein folding. Kinet Sci 301:1233–1235

Matouschek A, Kellis JT, Serrano L, Bycroft M, Fersht AR (1990) Transient folding intermediates characterized by protein engineering. Nature 346:440–445

Mayor U, Guydosh NR, Johnson CM, Grossmann JG, Sato S, Jas GS, Freund SM, Alonso DO, Dagget V, Fersht AR (2003) The complete folding pathway of a protein from nanoseconds to microseconds. Nature 421:863–867

Myers JK, Oas TG (2002) Mechanism of fast protein folding. Annu Rev Biochem 71:783–815

Onuchic JN, Luthey-Schulten Z, Wolynes PG (1997) Theory of protein folding: the energy landscape perspective. Annu Rev Phys Chem 48:545–600

Rhoades E, Gussakovsky E, Haran G (2003) Watching proteins fold one molecule at a time. Proc Natl Acad Sci USA 100:3197–3202

Schuler B, Lipman EA, Eaton WA (2002) Probing the free-energy surface for protein folding with single-molecule fluorescence spectroscopy. Nature 419:743–747

Shen CY, Kostic NM (1997) Kinetics of photoinduced electron-transfer reactions within sol-gel silica glass doped with zinc cytochrome c. Study of electrostatic effects in confined liquids. J Am Chem Soc119:1304–1312

Talaga DS, Lau WL, Roder H, Tang J, Jia Y, DeGrado WF, Hochstrasser RM (2000) Dynamics and folding of single two-stranded coiled-coil peptides studied by fluorescent energy transfer confocal microscopy. Proc Natl Acad Sci USA 97:13021–13026

Tanford C (1968) Protein denaturation. Adv Prot Chem 23:121–282

Weiss S (2000) Measuring conformational dynamics of biomolecules by single molecule fluorescence spectroscopy. Nat Struct Biol 7:724–729

Went HM, Benitez-Cardoza CG, Jackson SE (2004) Is an intermediate state populated on the folding pathway of ubiquitin? FEBS Lett 567:333–338

Zimmer M (2002) Green fluorescent protein (GFP): applications, structure, and related photophysical. Behav Chem Rev 102:759–781